Characterization and modelling of the boron-oxygen defect activation in compensated *n*-type silicon

J. Schön, T. Niewelt, J. Broisch, W. Warta, and M. C. Schubert
Fraunhofer Institute for Solar Energy Systems ISE, Heidenhofstr. 2, 79110 Freiburg, Germany

(Received 28 October 2015; accepted 12 December 2015; published online 28 December 2015)

A study of the activation of the light-induced degradation in compensated *n*-type Czochralski grown silicon is presented. A kinetic model is established that verifies the existence of both the fast and the slow components known from *p*-type and proves the quadratic dependence of the defect generation rates of both defects on the hole concentration. The model allows for the description of lifetime degradation kinetics in compensated *n*-type silicon under various intensities and is in accordance with the findings for *p*-type silicon. We found that the final concentrations of the slow defect component in compensated *n*-type silicon only depend on the interstitial oxygen concentration and on neither the boron concentration nor the equilibrium electron concentration n_0. The final concentrations of the fast defect component slightly increase with increasing boron concentration. The results on *n*-type silicon give new insight to the origin of the BO defect and question the existing models for the defect composition. © *2015 AIP Publishing LLC*.
[http://dx.doi.org/10.1063/1.4938569]

I. INTRODUCTION

Although the severe light-induced degradation (LID) of Czochralski (Cz) grown silicon due to the boron-oxygen defect (BO defect) has been studied for decades,[1–24] neither composition nor origin are clarified, yet. The efficiency of solar cells from *p*-type[8] and compensated *n*-type[25] Cz silicon can be reduced strongly due to activation of the BO defect during operation. The amount of LID is studied by means of an effective defect concentration N_t^*, which is calculated from excess charge carrier lifetime measurements after defect activation by illumination and after annealing in the dark—a process known to revert BO defects into a non-active state. Studies on boron doped Cz silicon have established an almost quadratic ($[O]^{1.9\pm0.1}$) relation of both BO defect components, i.e., fast-formed and slow-formed recombination center (FRC and SRC), on the concentration of interstitial oxygen O_i (e.g., in Refs. 6 and 8).

The study of LID in *p*-type silicon doped with boron and phosphorus (compensated silicon) provided further insights as well as vivid discussion on the composition of the defect.[12,14,24] It was found that the concentration of the SRC scales with the net doping concentration $N_{net} = [B_s^-] - [P_s^+]$ resembling the equilibrium hole concentration p_0 (e.g., Ref. 10). As a consequence, a new defect model for SRC based on a B_iO_2 complex was proposed.[12,14] Further studies on material co-doped with boron and gallium by Forster *et al.*[18] revealed an influence of the B_s concentration. This finding contradicted the prediction of the B_iO_2 model and lead to a revised B_i model by Voronkov *et al.*[24]

Studies of compensated *n*-type silicon allow assessing the influence of charge carrier concentrations and boron content with an additional degree of freedom due to the minority character of holes in *n*-type silicon. Voronkov *et al.*[24] took advantage of this possibility and developed a kinetic model and a Shockley-Read-Hall (SRH) parametrization for the fast BO defect. They concluded that the fast BO defect component is not involving a B_i and might thus be composed of substitutional boron as suggested by Bothe and Schmidt.[8] In contrast to *p*-type silicon, the kinetics of LID in compensated *n*-type silicon depended strongly on the illumination intensity. The degradation kinetics in compensated *n*-type wafers was also studied by Rougieux *et al.*[16,26] who concluded from their lifetime measurements that the BO defect in *n*-type silicon was formed in a single-step process. However, the slow BO defect component in compensated *n*-type silicon has been evidenced, recently.[27] In addition, a SRH parameterization of the SRC was proposed where the recombination activity is associated to a two-level defect center[27] instead of the former SRH description with two independent SRH defects.[7,28]

In this work, we analyze the kinetics of LID in a comprehensive study on compensated *n*-type silicon. The high charge carrier lifetime of the samples and the different experimental setups allow us to study both the FRC and the SRC related to BO-defects, as known from *p*-type silicon. Furthermore, we present a kinetic model based on parameters in *p*-type silicon, the findings for the FRC in *n*-type silicon,[24] and the recent SRH parameterization of the SRC.[27] The model is compared with the measured lifetime evolution of samples under different illumination conditions and yields the effective concentrations of FRC and SRC. The concentrations are related to sample properties and the resulting implications on the mechanism and origin of LID are discussed.

II. EXPERIMENTAL DETAILS

The study is based on 23 *n*-type wafers from different positions of two compensated Cz crystals, one grown from upgraded metallurgical grade (*umg*) silicon feedstock and one grown from electronic grade feedstock with phosphorus

and boron doping. The dopant concentrations [B] and [P] in the wafers were calculated from the concentrations in the melt applying Scheil's equation[29] and checked by dopant concentration measurements.[30] The net doping concentration n_0 is calculated from resistivity measurements considering the reduced mobility by compensation as suggested in Ref. 23. The interstitial oxygen concentration was extrapolated from FTIR measurements at different ingot heights. In the wafers from the *umg* ingot, [B] increases with ingot height from $1.2 \times 10^{16}\,\mathrm{cm}^{-3}$ to $1.6 \times 10^{16}\,\mathrm{cm}^{-3}$, n_0 from $0.5 \times 10^{15}\,\mathrm{cm}^{-3}$ to $16.5 \times 10^{15}\,\mathrm{cm}^{-3}$, and $[O_i]$ decreases from $7.4 \times 10^{17}\,\mathrm{cm}^{-3}$ to $5.7 \times 10^{17}\,\mathrm{cm}^{-3}$. The higher boron concentration in the melt of the electronic grade ingot leads to [B] from $5 \times 10^{16}\,\mathrm{cm}^{-3}$ to $10 \times 10^{16}\,\mathrm{cm}^{-3}$ and n_0 from $1.2 \times 10^{16}\,\mathrm{cm}^{-3}$ to $2.8 \times 10^{16}\,\mathrm{cm}^{-3}$, whereas $[O_i]$ decreases slightly from $7.6 \times 10^{17}\,\mathrm{cm}^{-3}$ to $7.0 \times 10^{17}\,\mathrm{cm}^{-3}$ in the analyzed (*n*-type) part of the ingot. After saw damage removal and cleaning, the wafers underwent a phosphorus diffusion from both sides. The diffused regions were etched off and a silicon-rich oxynitride stack[31] was deposited by PECVD. The surface passivation was activated in a short high temperature step with a peak temperature of 700 °C. Sample thicknesses between 160 and 175 μm were measured after processing. Before light soaking, the samples were annealed for 30 min at 250 °C to prepare the inactive BO defect state.

To investigate the influence of different injection conditions on the degradation process without influences of sample temperature, all samples were degraded on cooled sample stages at 25 °C but under varied illumination intensities. The different illumination intensities of the halogen lamps were measured with a solar cell and converted into sun equivalents. The sun equivalent was defined with the solar cell current under illumination with 1013 W/m^2 AM 1.5G spectrum. A set of samples was degraded under illumination equivalent to 0.7 (±0.1) suns provided by halogen lamps for 95 h. A second set of samples was first illuminated at 0.023 (±0.01) sun equivalents for 99 days. Five of these samples were subsequently illuminated at 0.5 (±0.05) sun equivalents for 80 h and at 1 (±0.1) sun equivalent for 67 h. Three wafers were further degraded at higher illumination intensity of up to 10 sun equivalents. Lifetime evolution of the samples was monitored using QSSPC lifetime measurements to study the kinetics of the lifetime degradation. The illumination was interrupted for these measurements and sample positions were randomized to minimize possible detrimental effects due to intensity variations of the setup.

In addition to the *ex situ* experiment with halogen lamps, a sample was degraded under 790 nm cw laser illumination and the lifetime was measured *in situ* with modulated photoluminescence measurements[32] in the first few hours. This provided high temporal resolution in the early stage of the degradation and excludes influences of the illumination interruptions on the degradation process. Later measurements at this sample were conducted *ex situ*.

Most lifetime measurements in this study were conducted with a Sinton Instruments WCT_120 QSSPC Lifetime tester.[33] We utilized a correction for compensated silicon suggested by Forster *et al.*[23] by determining an apparent doping concentration N_{app} that reproduces the actual carrier mobility sum with the model of Dannhäuser and Krausse[34,35] for the lifetime evaluation. This was done by calculating the actual charge carrier mobility sum with the recent charge carrier mobility model by Schindler *et al.*[36] and adjusting N_{app} to reproduce it. While this approach can be exact for a single injection level, it cannot avoid slight deviations due to the changing injection dependence of the mobility sum with variation of the doping concentration. An assessment of this uncertainty for various doping concentrations was done and the detrimental influence was minimized for every sample. We estimate the additional uncertainty in the lifetime measurements due to the compensation effect on charge carrier mobilities to be in the order of a few percent. If not stated otherwise, the lifetimes in this study were evaluated at a fixed minority carrier density of 0.3 times the respective sample's net doping concentration n_0. This allows improved comparability compared with a fixed minority carrier density and was found to be a convenient injection level for most samples.

III. DEGRADATION KINETICS

A. Measurements of SRC in n-type silicon

Severe reduction of the minority charge carrier lifetimes was observed for all samples subjected to light soaking. Some samples were annealed after final degradation and charge carrier lifetimes of up to 3 ms were measured. Thus, a significant degradation of the samples due to stable defects can be excluded. The *in situ* modulated photoluminescence measurements during LID with a laser yielded a high density of lifetime measurements in the early stage of the degradation process. The resulting lifetime curve clearly shows a two-stage progression of the lifetime degradation, as demonstrated in Figure 1 (red dots).

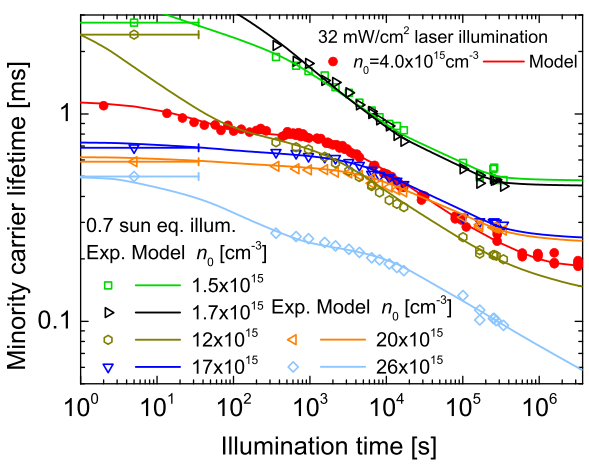

FIG. 1. The symbols denote the measured effective charge carrier lifetime at $\Delta n = 0.3 \times n_0$ (sample with $n_0 = 4.0 \times 10^{15}\,\mathrm{cm}^{-3}$: $\Delta n = 0.25 \times n_0$ and sample with $n_0 = 26 \times 10^{15}\,\mathrm{cm}^{-3}$: $\Delta n = 0.06 \times n_0$) for different *n*-type samples under halogen lamp illumination with 0.7 sun equivalents or laser illumination with 32 mW/cm^2 (sample with $n_0 = 4.0 \times 10^{15}\,\mathrm{cm}^{-3}$). The modulated photoluminescence method[32] allows for fast *in situ* lifetime measurements at the beginning of the degradation process under laser illumination and proves the two-step degradation, resembling the behavior of *p*-type silicon. The different initial lifetimes of the samples can be explained by the different Auger recombination and a significant τ_{other} for three samples. The lines are a result of the kinetic model described in Section III B.

The degradation experiment with halogen lamps with illumination intensity of 0.7 sun equivalents and *ex situ* QSSPC measurements involves more samples. A representative selection of these lifetime measurements is shown in Figure 1. We found that the fast degradation process under 0.7 sun equivalents halogen illumination is almost completed before the second QSSPC measurement. The effective degradation time between the annealing and the first QSSPC measurement faces uncertainty (as indicated with the large error bars) and may vary from sample to sample due to light soaking during sample handling after annealing and during the QSSPC measurements themselves. This hinders the differentiation between lifetime limitation due the fast component and other limitations. The observed degradation curves differ significantly from the exponential evolution known from *p*-type silicon and depend on the charge carrier concentration which decreases during LID. The injection dependence of the lifetimes was found to change with proceeding degradation which is an evidence of a two-step degradation with two different defects, i.e., FRC and SRC.

B. Modelling the activation kinetics of BO defects in n-type silicon

We modeled the activation kinetics of the BO defects in order to separate the two degradation processes and study their characteristics. In the model, we use the same illumination intensity for all samples degraded together. The reflectivity of the samples for the illumination spectrum is taken into account to determine the hole concentration. The key assumptions of our model are that both processes occur independently and that their underlying processes are activated by charge carrier injection and thus depend on minority charge carrier concentration. We assume four recombination channels: FRC, SRC, Auger recombination, and an injection independent τ_{other}. Activation kinetics and recombination activity of the FRC are assumed as described in Ref. 17. The defect activation rate r in compensated n-type silicon:[17]

$$r_{FRC} = 350\,\mathrm{s}^{-1} \times e^{\left(-\frac{0.23\,\mathrm{eV}}{k_B T}\right)} \times \left(\frac{p}{10^{16}\,\mathrm{cm}^{-3}}\right)^2 \times \frac{p}{p + 2 \times 10^{14}\,\mathrm{cm}^{-3}}, \tag{1a}$$

$$r_{SRC} = 6500\,\mathrm{s}^{-1} \times e^{\left(-\frac{0.475\,\mathrm{eV}}{k_B T}\right)} \times \left(\frac{p}{10^{16}\,\mathrm{cm}^{-3}}\right)^2, \tag{1b}$$

is calculated by applying the quadratic dependence on the hole concentration[18] p and the rate coefficients known from *p*-type silicon.[8] The factor $p/(p + 2 \times 10^{14}\,cm^{-3})$ was added by Voronkov *et al.*[17] to gain an optimized description of the degradation kinetics of the FRC in compensated *n*-type silicon. In our experiment, the factor f influences the fitting quality only for samples with n_0 larger than $2.5 \times 10^{16}\,\mathrm{cm}^{-3}$ and for these two samples the factor found by Voronkov *et al.* works well.

During the degradation process, the injection dependent lifetime due to the FRC and SRC is described as two two-level defects.[17,27] The Auger recombination at the evaluated injection level of the measurement and during the degradation process is calculated using the Richter model.[37] For six of the samples, we found a significantly small τ_{other} of ~1 ms (e.g., red, orange, and blue curves in Fig. 1). This lifetime limitation might be due to surface recombination or other defects. However, most likely the reason for the significantly small τ_{other} is an unintentional activation of the FRC before the first measurement or an incomplete deactivation process. Due to the significantly small τ_{other} with unknown injection dependence and the discussed uncertainties in the setup, a clear analysis of the FRC is not possible for these samples. However, even for these samples, the influence of the unknown injection dependence of τ_{other} can be neglected in the relevant lifetime measurements for the SRC analysis.

For a satisfying modelling of the lifetime degradation in different *n*-type samples, the exact injection dependent FRC and SRC lifetime for the calculation of the hole concentration p at the respective degradation evolution is essential due to the quadratic dependency of the kinetics of FRC and SRC activation on the hole concentration.

Despite the missing knowledge of the absolute number of the BO capture coefficients, fits using the electrical descriptions of the FRC[17] and SRC[27] can provide quantities proportional to the true defect concentrations, resembling the N_t^* approach known from *p*-type silicon. These quantities are injection level independent and resemble the product of the actual concentration N_t and one capture coefficient. This allows a comparison of the defect concentration of differently doped samples and even between *p*- and *n*-type samples.

The saturated N^*_{tFRC} and N^*_{tSRC} as well as τ_{other} are fitted to the measured lifetime evolution shown in Figure 1, i.e., at an injection level of $0.3 \times n_0$ for most samples. The measured lifetime evaluation during degradation at 0.5 and 0.7 sun equivalents can be well described by the fitting of saturated N^*_{tFRC} and N^*_{tSRC} (see Figure 1). From the modelled lifetime, we can conclude that most samples are not fully degraded after 95 h.

In a next step, we tested our model with literature data (Fig. 2). We chose the data for compensated *n*-type silicon at 60 °C from which Rougieux *et al.*[26] concluded that the degradation process in *n*-type silicon is a one step process. The

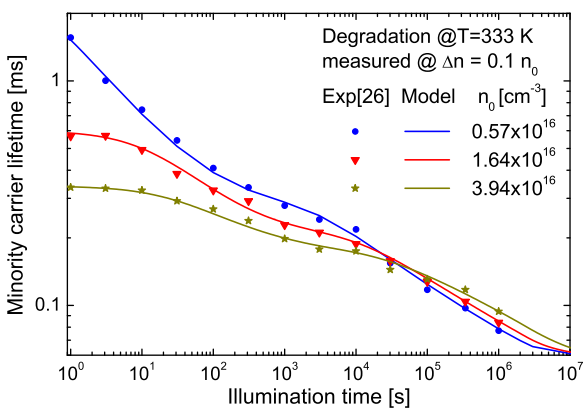

FIG. 2. Measured lifetime degradation from Rougieux *et al.*[26] during illumination with 60 mW/cm^{-2} at 60 °C in comparison with the modeled lifetime. The lifetime of the three samples with different net doping concentration was measured at an injection level of $\Delta n = 0.1 \times n_0$.

presented two-step model is in good agreement with the measured data. This supports our model and the activation energies for the defect activation found for the defects in *p*-type silicon.[8]

C. Multistep degradation

In Figure 3, the lifetime degradation under halogen illumination with an intensity of 0.023 sun equivalents followed by a degradation at an intensity of 0.5 sun equivalents and at an intensity of 1 sun equivalents is compared with the modeled lifetime fitting the saturated N^*_{tFRC}, N^*_{tSRC}, and τ_{other} for every sample. Samples with lower net doping have higher lifetime and degrade faster than samples with higher n_0. The simple comparison of the lifetime after degradation at one illumination (Figure 3) gives the impression that the defect concentration increases with illumination intensity as it was concluded in Ref. 16. However, the differences in the final lifetime are only due to incomplete degradation as the whole lifetime evolution of a sample can be described with the same saturated N^*_{tFRC} and N^*_{tSRC} for all illumination intensities.

We observe saturation for some samples under illumination with 1 sun equivalent. The samples with a net doping of $2 \times 10^{15}\,\mathrm{cm}^{-3}$ and $4 \times 10^{15}\,\mathrm{cm}^{-3}$ that underwent the multistep degradation were further illuminated at 2 sun equivalents (~100 h), 5 sun equivalents (~50 h), and 10 sun equivalents (~60 h, only sample with $n_0 = 2 \times 10^{15}\,\mathrm{cm}^{-3}$). As expected from the model, the samples degrade only slightly: The lifetime decreases by 12% for the sample with $n_0 = 2 \times 10^{15}\,\mathrm{cm}^{-3}$ and by 17% for the sample with $n_0 = 4 \times 10^{15}\,\mathrm{cm}^{-3}$. In contrast, the sample with $n_0 = 28 \times 10^{15}\,\mathrm{cm}^{-3}$ degrades further during illumination at 10 sun equivalents (360 h) to a lifetime of 58 μs (modelled 47 μs).

IV. CONCENTRATION OF FAST AND SLOW BO DEFECT COMPONENTS

In combination with the injection dependent parameterizations of the defect lifetimes of the FRC by Voronkov *et al.*[17] and the electrical description of SRC established in Ref. 27, the model also allows to predict equilibrium lifetimes and assess the saturated effective defect concentrations N^*_{tFRC} and N^*_{tSRC} from non-saturated measurement curves. Due to the long timescales of the degradation effect in *n*-type silicon (note the logarithmic timescales in the figures), these crucial parameters are not experimentally accessible in many cases. For further analyses, the saturated defect concentrations N^*_{tFRC} and N^*_{tSRC} are divided by $[O_i]^2$ due to the quadratic O_i dependency known for *p*-type silicon[8] and the FRC in *n*-type silicon.[17]

The normalized concentrations of the slow component obtained by fitting the model presented in Section III B with the measured lifetime evolutions (see Figs. 1–3) are shown in Figure 4 in dependency of the net doping concentration of the samples. The determined saturated N^*_{tSRC} vary by a factor of 3, but no significant dependency from the net doping or boron concentration is observed. This is remarkable as the final degraded lifetimes in Figs. 1–3 decrease with n_0. The observed differences in the degraded lifetimes can be related to the different injection dependence of the lifetime. For a given defect concentration, the measured lifetime for different doping concentrations varies even when evaluated at a constant ratio of minority to majority carriers. The variations in the extracted N^*_{tSRC} are probably due to uncertainties in the determined samples parameters, mainly $[O_i]$ and n_0.

For some of our samples, a clear determination of the effective concentration of the fast component N^*_{tFRC} is not possible due to the significantly small τ_{other} for these samples. Figure 5 shows the normalized concentrations of the fast component obtained by the fitting procedure in dependency of the net doping concentration for samples that allow an unambiguous determination of N^*_{tFRC}. We see a slight increase of the saturated N^*_{tFRC} with the net doping concentration. However, this slight increase is rather insignificant compared with the scattering of the data, especially if the N^*_{tFRC} of one sample group are compared.

V. DISCUSSION

The lifetime in the multi-step degradation can be reproduced with one saturated N^*_{tFRC} and one saturated N^*_{tSRC} for

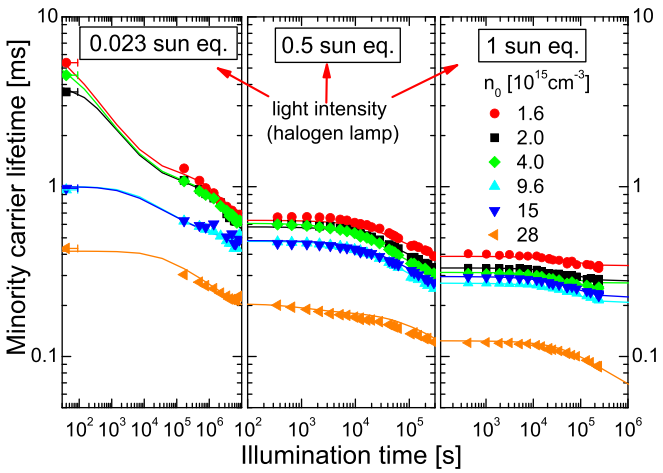

FIG. 3. Lifetime evolution at $\Delta n = 0.3 \times n_0$ (sample with $n_0 = 28 \times 10^{15}\,\mathrm{cm}^{-3}$: $\Delta n = 0.06 \times n_0$) under long-term illumination of increasing intensity. Higher intensity illumination is found to accelerate the degradation process. The lines are the results of the kinetic model described in Section III B.

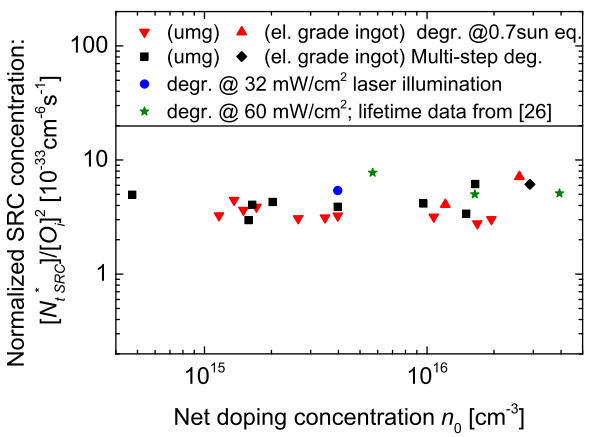

FIG. 4. Normalized concentrations of the saturated slow component N^*_{tSRC} obtained by fitting the model to the measured lifetime evolutions (see Figures 1–3) in dependency of the net doping concentration of the samples.

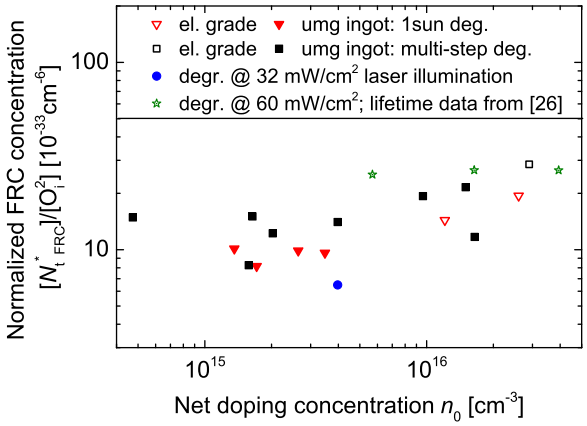

FIG. 5. Normalized concentrations of the saturated fast component N^*_{tFRC} obtained by fitting the model to the measured lifetime evolutions (see Figures 1–3) in dependency of the net doping of the samples.

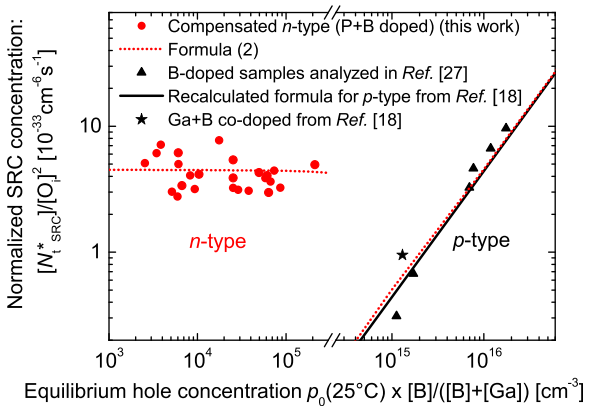

FIG. 6. Normalized concentrations of the slow component obtained by fitting the model to the measured lifetime evolutions in the *n*-type samples (see Figures 1–3) in dependency of the equilibrium hole concentration at room temperature times the ratio of boron and acceptors concentration. In addition, normalized N^*_{tSRC} for the *p*-type samples from Ref. 27, the Ga + B co-doped sample from Ref. 18 and the known dependency for *p*-type silicon are shown. The SRC concentrations for *p*- and *n*-type samples can be reproduced with formula (2) (for the red dotted line, we use $n_i(T_n) = 2 \times 10^{12}\,\mathrm{cm}^{-3}$ and $n_i(T_p) = 2 \times 10^{13}\,\mathrm{cm}^{-3}$).

all illumination intensities. Thus, we conclude that the saturated N^*_{tFRC} and N^*_{tSRC} do not depend on the illumination intensity, i.e., actual electron or hole concentration. This finding is further supported by the invariance of the lifetime under illumination with 2–10 sun equivalents after complete degradation at 1 sun equivalent.

Additionally, our results confirmed the quadratic $[O_i]$ dependency, i.e., the involvement of two interstitial oxygen atoms in the defect formation, also for the SRC in *n*-type silicon. The concentration of the saturated N^*_{tSRC} in *n*-type silicon is independent of the net doping concentration n_0 (see Figure 4). Following the argumentation by Voronkov *et al.*,[17,24] we can exclude both proposed B_i models,[17,24] due to the dominating negative charge state of B_i in *n*-type silicon that should result in a linear dependence of the saturated N^*_{tSRC} on the net doping n_0.

In former experiments with *p*-type silicon, N^*_t was extracted from the inverse lifetimes measured at a fixed fraction of p_0 (usually $0.1 \times p_0$). In general, this approach is not applicable for a two-level defect due to the influence of the net doping p_0 on the injection dependency of the lifetime. The approach, however, gives a good approximation for *p*-type samples because both, FRC and SRC, are dominated by their deep defect levels over a broad injection range in *p*-type silicon according to the two-level defect parameterizations from Refs. 17 and 27. As a consequence, the SRC concentrations of *p*-type samples evaluated with the new two-level SRH parameters are in good agreement with the corrected curve[18] from Bothe and Schmidt[8] (see Figure 6). For the comparison of our data and *p*-type data from the literature, it has to be considered that the parameterizations are normalized to different capture cross sections and the two-level parameterizations result in effective defect concentrations independent of the injection level. The normalization to the electron capture cross section of the donor level α_{n1} in the literature instead of the normalization to the hole capture cross section α_{p1} results in a factor of $\alpha_{p1}/\alpha_{n1} = 0.105$ (Ref. 27) and the evaluation at $0.1 \times p_0$ instead of the evaluation at low injection level to a factor of 1.9 (Ref. 7). Thus, we multiplied the literature data by 0.2 for the graph in Figure 6.

Figure 6 shows that depending on the doping concentration the SRC concentration in *p*-type silicon can be higher or lower than in *n*-type silicon. This complicates the description of saturated N^*_{tSRC} as a function of charge carrier concentrations and indicates a generation process of the defect with several defect precursors that were formed at different temperatures during cooldown. As a first step to discuss the composition of the SRC, we propose an empiric description of saturated N^*_{tSRC} which is valid in *n*-type silicon as well as uncompensated[8] and compensated[18] *p*-type silicon. The dotted red line in Figure 6 has the form:

$$N^*_{tSRC} = p(T_p) \times 4.3 \times 10^{-33}\mathrm{cm}^{-6}\mathrm{s}^{-1} \times \left(1 \times 10^{-16}\mathrm{cm}^3 + \frac{n(T_n)}{(n_i(T_p))^2}\right) \times \frac{[B_S]}{[Acc_S]} \times [O_i]^2. \quad (2)$$

$[B_s]$ denotes the concentration of substitutional boron and $[Acc_s]$ denotes the concentration of all acceptors. $p(T_p)$ is the hole concentration during cooling down at temperature T_p at which either a positively charged species is involved in the formation of a defect precursor or the concentration of a positively charged species is frozen in retaining its interaction potential. Similar to that, the dependency on the concentration of electrons $n(T_n)$ at temperature T_n plus a constant indicates a species that is involved in the negative and neutral state in the defect formation, e.g., by interaction with given precursors. The temperatures T_p and T_n have to be in the extrinsic regimes, i.e., $n_i(T_{p/n}) < p_0$ or $n_i(T_{p/n}) < n_0$, to explain the p_0 dependence of *p*-type samples. Furthermore, a consistent fit of all measured data in Figure 6 is only achieved if the intrinsic charge carrier concentration n_i at T_p is one or more orders of magnitude higher than $n_i(T_n)$, i.e., the temperature T_p at which the positive species interacts is higher than the temperature T_n.

The necessity of boron in the samples could be explained as follows: during cooldown, a precursor X_{SRC} binds to

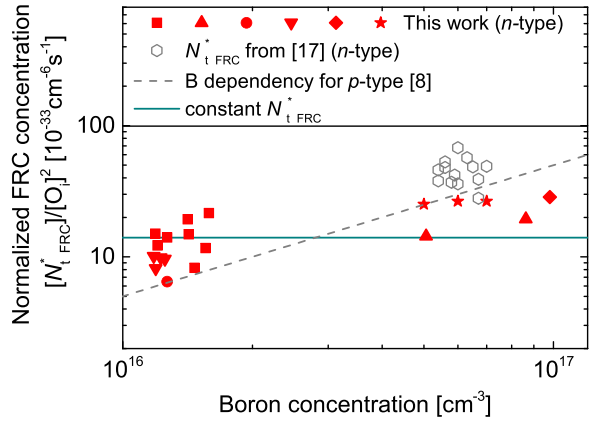

FIG. 7. Normalized concentrations of the fast component obtained by fitting the model to the measured lifetime evolutions in dependency of the boron concentration of the samples. For comparison the saturated N^*_{tFRC} obtained from compensated *n*-type samples in Ref. 17 and the saturated N^*_{tFRC} that is expected for *p*-type silicon with the respective boron concentration[8,17] are shown.

substitutional acceptors but is not active. Then, the concentration of inactive SRC bound to substitutional boron (B_s) is independent of [B_s] as long as [B_s] $\gg$ [X_{SRC}]. An indifferent binding of X_{SRC} with substitutional acceptors (Acc_s) then explains the reduced defect concentration upon replacement of B with Ga at fixed p_0 exhibited by Forster *et al.*[18]

The saturated concentration of the fast component N^*_{tFRC} in dependency of the boron concentration is shown in Figure 7. Voronkov *et al.*[17,24] predict that the saturated N^*_{tFRC} is proportional to the boron concentration which is caused by a B_sO_2 defect. In our data, the saturated N^*_{tFRC} increases only slightly with the boron concentration. In addition, our results are in accordance with the saturated concentrations of N^*_{tFRC} in dependency of the boron concentration for *p*-type silicon. However, the large scattering of the saturated N^*_{tFRC} impedes a proof or disproof of the predicted linear dependency on the boron concentration. In analogy to the SRC, N^*_{tFRC} might also be constant in *n*-type silicon as indicated by the solid line in Figure 7.

Voronkov *et al.*[17] found higher saturated N^*_{tFRC} compared with our experiments. However, the influence of SRC was neglected in their analysis. According to our model, after full activation of the FRC, 15% to 50% of the lifetime degradation are related to SRC, which may cause an overestimation of N^*_{tFRC} in Ref. 17. Also, the absence of a phosphorus diffusion step in Ref. 17 can cause higher effective defect concentrations. Such processes are known to impact the defect concentration in *p*-type silicon and might also affect the defect in *n*-type silicon as well (e.g., in Ref. 5).

VI. CONCLUSIONS

The presented kinetic model for the slow and fast BO defect describes the measured lifetime degradation in all compensated *n*-type samples with strongly varying phosphorus and boron concentrations. Key features of the kinetic model are the quadratic dependency on the hole concentration known from *p*-type silicon[17,18] and the electrical description of both defects as a two-level defect.[17,27] Thus, the consistent kinetic description of the SRC supports the new electrical description of the SRC as a two-level defect center. The fitted concentrations of the SRC in the analyzed *n*-type silicon are independent of the net doping in n_0 and the boron concentration. Thus, an involvement of interstitial boron atoms in the defect formation is rather unlikely. Previous models on the composition of the SRC[17,24] are contradicted by our results.

ACKNOWLEDGMENTS

The authors would like to thank V. V. Voronkov and R. Falster from SunEdison for fruitful discussions. This work was supported by the German Federal Ministry for the Environment, Nature Conservation and Nuclear Safety within BORNEO project (Grant No. 0325450B).

[1]J. Schmidt, A. G. Aberle, and R. Hezel, paper presented at the 26th IEEE Photovoltaic Specialists Conference, 1997, pp. 13–18.
[2]S. Rein, T. Rehrl, W. Warta, S. W. Glunz, and G. Willeke, paper presented at the 17th European Photovoltaic Solar Energy Conference, Munich, Germany, 2001.
[3]K. Bothe, J. Schmidt, and R. Hezel, paper presented at the 29th IEEE Photovoltaics Specialists Conference, New Orleans, Louisiana, USA, 2002.
[4]S. Rein and S. W. Glunz, Appl. Phys. Lett. **82**(7), 1054–1056 (2003).
[5]K. Bothe, R. Hezel, and J. Schmidt, in *Gettering and Defect Engineering in Semiconductor Technology*, edited by H. Richter and M. Kittler (Trans Tech Publications Ltd., Zurich-Uetikon, 2004), Vols. 95–96, pp. 223–228.
[6]K. Bothe, R. Sinton, and J. Schmidt, Prog. Photovoltaics **13**, 287–296 (2005).
[7]S. Rein, *Lifetime Spectroscopy: A Method of Defect Characterization in Silicon for Photovoltaic Applications*, 1st ed. (Springer, Berlin, Heidelberg, 2005).
[8]K. Bothe and J. Schmidt, J. Appl. Phys. **99**(1), 013701 (2006).
[9]A. Herguth, G. Schubert, M. Kaes, and G. Hahn, paper presented at the 4th WCPEC, Hawaii, USA, 2006.
[10]R. Kopecek, J. Arumughan, K. Peter, E. A. Good, J. Libal, M. Acciarri, and S. Binetti, paper presented at the 23rd European Photovoltaic Solar Energy Conference, Valencia, 2008.
[11]H. Savin, M. Yli-Koski, and A. Haarahiltunen, Appl. Phys. Lett. **95**(15), 152111 (2009).
[12]D. Macdonald, F. Rougieux, A. Cuevas, B. Lim, J. Schmidt, M. Di Sabatino, and L. J. Geerligs, J. Appl. Phys. **105**, 093704 (2009).
[13]T. Schutz-Kuchly, J. Veirman, S. Dubois, and D. R. Heslinga, Appl. Phys. Lett. **96**, 093505 (2010).
[14]V. V. Voronkov and R. Falster, J. Appl. Phys. **107**, 053509 (2010).
[15]D. Macdonald, A. Liu, A. Cuevas, B. Lim, and J. Schmidt, Phys. Status Solidi A **208**(3), 559–563 (2011).
[16]F. E. Rougieux, M. Forster, D. Macdonald, A. Cuevas, B. Lim, and J. Schmidt, IEEE J. Photovoltaics **1**(1), 54–58 (2011).
[17]V. V. Voronkov, R. Falster, K. Bothe, B. Lim, and J. Schmidt, J. Appl. Phys. **110**(6), 063515 (2011).
[18]M. Forster, E. Fourmond, F. E. Rougieux, A. Cuevas, R. Gotoh, K. Fujiwara, S. Uda, and M. Lemiti, Appl. Phys. Lett. **100**(4), 042110 (2012).
[19]T. U. Naerland, H. Angelskar, M. Kirkengen, R. Sondena, and E. S. Marstein, J. Appl. Phys. **112**(3), 033703 (2012).
[20]V. V. Voronkov, R. Falster, K. Bothe, and B. Lim, Energy Procedia **38**, 636–641 (2013).
[21]T. U. Naerland, H. Haug, H. Angelskar, R. Sondena, E. S. Marstein, and L. Arnberg, IEEE J. Photovoltaics **3**(4), 1265–1270 (2013).
[22]K. Fraser, D. Blanc-Pelissier, S. Dubois, J. Veirman, F. Tanay, and M. Lemiti, Energy Procedia **38**, 542–550 (2013).
[23]M. Forster, P. Wagner, J. Degoulange, R. Einhaus, G. Galbiati, F. E. Rougieux, A. Cuevas, and E. Fourmond, Sol. Energy Mater. Sol. C **120**, 390–395 (2014).
[24]V. V. Voronkov and R. Falster, in *Gettering and Defect Engineering in Semiconductor Technology Xv*, edited by J. D. Murphy (Trans Tech Publications Ltd., Stafa-Zurich, 2014), Vols. 205–206, pp. 3–14.
[25]J. Broisch, J. Schmidt, J. Haunschild, and S. Rein, Energy Procedia **55**, 526–532 (2014).
[26]F. E. Rougieux, B. Lim, J. Schmidt, M. Forster, D. Macdonald, and A. Cuevas, J. Appl. Phys. **110**(6), 063708 (2011).
[27]T. Niewelt, J. Schön, J. Broisch, W. Warta, and M. C. Schubert, Phys. Status Solidi (RRL) **9**, 692–696 (2015).

[28]J. Schmidt and A. Cuevas, J. Appl. Phys. **86**(6), 3175–3180 (1999).
[29]E. Scheil, Z. Metall. **34**, 70–72 (1942).
[30]J. Broisch, J. Haunschild, and S. Rein, IEEE J. Photovoltaics **5**(1), 269–275 (2015).
[31]J. Seiffe, L. Gautero, M. Hofmann, J. Rentsch, R. Preu, S. Weber, and R. A. Eichel, J. Appl. Phys. **109**(3), 034105 (2011).
[32]J. Giesecke, M. C. Schubert, D. Walter, and W. Warta, Appl. Phys. Lett. **97**(9), 092109 (2010).
[33]R. A. Sinton and A. Cuevas, Appl. Phys. Lett. **69**(17), 2510–2512 (1996).
[34]F. Dannhäuser, Solid-State Electron. **15**(12), 1371–1375 (1972).
[35]J. Krausse, Solid-State Electron. **15**(12), 1377–1381 (1972).
[36]F. Schindler, M. Forster, J. Broisch, J. Schoen, J. Giesecke, S. Rein, W. Warta, and M. C. Schubert, Sol. Energy Mater. Sol. C **131**, 92–99 (2014).
[37]A. Richter, S. W. Glunz, F. Werner, J. Schmidt, and A. Cuevas, Phys. Rev. B **86**(16), 165202 (2012).